

# **Grated Compressor Modeling**

**Jeremy Chang**

## *Grating Compressor Modeling*

Jeremy Chang  
Penfield High School  
Advisor: Mark Guardalben

University of Rochester  
Laboratory for Laser Energetics  
Summer High School Research Program

### **Abstract**

In order to avoid laser-induced damage to optical components during amplification of a short laser pulse, the pulse often is first stretched in time to reduce its peak power, amplified, and then recompressed. High peak irradiance is attained when the laser beam is subsequently focused onto a laser fusion target. In a laser system, currently under construction, large diffraction gratings will be used in a precise alignment in order to provide pulse compression. Misalignment of the diffraction gratings that comprise the grating compressor can lead to less than optimal pulse compression and reduced ability to focus the beam owing to residual angular dispersion of the pulse spectrum. A computer program was used to model the grating compressor system. The effects of grating alignment errors on the compressed pulse and focused beam were found. A pulse can be broadened from the transform limit of 606 fs to the tolerance limit of 1 ps, by errors in the alignment of diffraction gratings of 75  $\mu\text{rad}$  of tilt, 250  $\mu\text{rad}$  of tip, 450  $\mu\text{rad}$  of rotation, and 6 mm of distance mismatch. The requirement of 80% encircled energy in an area of radius 10  $\mu\text{m}$  is met for all errors corresponding to the 1 ps tolerance limit.

## I. Introduction

### 1.1 Grating Compressors

Since amplification of a short laser pulse can prove to be difficult and damaging to subsequent optics, a short laser pulse must be stretched in time before it is amplified and then recompressed. This process is known as Chirped Pulse Amplification (CPA)[1]. A stretched pulse will not damage optics, because the energy is spread out over time, which means it has a low intensity. Amplification of the pulse increases the amount of energy,

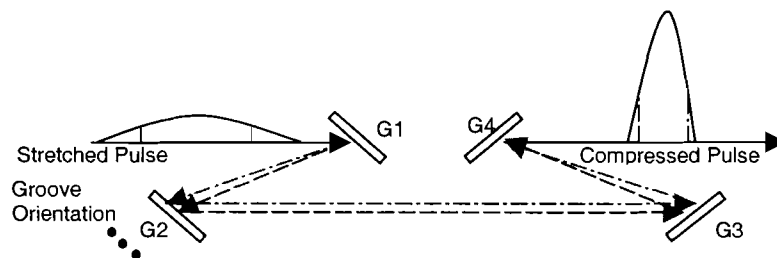


**Figure 1.1 A Four-Grating Compressor System** – A stretched laser pulse is propagated through a system of four diffraction gratings. Each frequency, shown here as the dotted line and dashed line, is diffracted at a different angle. This disparity in the angle of diffraction causes a path-length difference from one frequency to the next, which in turn creates a shift in time of some of the frequencies.

but does not raise the intensity over a level that would damage an optic. After amplification has been completed the laser pulse is passed through a system of four gratings, known as a grating compressor, in order to compress the pulse. This compression increases the intensity of the pulse by compressing it in time in order to heat the fusion target.

A grating compressor has the ability to shift the frequencies that compose a laser pulse in time causing a shift in time [2]. This shift is caused by the path-length difference from one frequency to the next. Since the frequencies towards the beginning of the pulse travel a longer distance, the pulse is compressed. Such compression allows a pulse to have a high intensity allowing the fusion target to heat up in a very short period of time.

A misalignment in the diffraction gratings, however, can cause the pulse to broaden from the transform limit, which is the compressed pulse for a perfect grating alignment.

Some misalignments cause angular dispersion in the laser beam. A number of definitions for angular dispersion are used. It can be described as either the angle between the orientation of the frequencies or the angle between the phase fronts of the frequencies [3]. Although these definitions may seem similar, they account for different phenomena in pulse and are therefore distinctly different. Angular dispersion between the phase fronts causes a wave front tilt, which causes temporal broadening of a spatially integrated temporal pulse. Angular dispersion in the orientation of the frequencies similarly accounts for a smearing in the far field of a beam.

## **1.2 Modeling**

The grating compressor was modeled, in order to find the margin of error that will be acceptable in the alignment of the diffraction gratings. An input beam of diameter 42 cm was used in the modeling in order to collect the data. The transform limit of 606 fs was the point of comparison from which the errors of each grating was found. The same input beam, composed of 451 rays was used throughout the experiment, and only the distance between gratings and orientation of gratings were changed. Several grating misalignments were run in order to derive a relationship between broadening and grating error. The tolerance limit was then found after extrapolating a line of best fit, and the result was then tested.

## II. Methodology

### 2.1 MANTARAY

In order to understand the effects of misalignment errors in the diffraction gratings on the pulse shape, a computer program MANTARAY was developed. Mantaray is a ray trace program. Each ray is diffracted through a component method and propagated through the grating compressor and then undergoes a Fourier Transform. This FFT allows the beam to be converted into a far field where spatial smearing can be seen. This yields information about the beam after compression both spatially and temporally.

The program is run from a configuration file, which has twelve lines. Line 3 calls a grating input file that is in the .mro file format. Within this file the optics are defined. A typical diffraction grating would be defined as: a diffraction-grating, x-y-z position, x-y-z orientation, rho/pi rotation, size, groove spacing, and back-behavior. The optics, which is used to find the far field, is also defined in the .mro file, and given a position, orientation, and grating size. Rays that fail to propagate through the system are written to a .txt file. After a run is completed another .txt file is created which stores information concerning the rays final position, time, orientation, and accumulated phase.

The running of the central ray preceded all runs. This allowed the orientation of the central ray to be found, and the optic to be set anti-parallel to the central beam. The user is prompted for the number of angles to be used in creating the encircled energy diagram. A run of the full beam then followed giving a plot of the temporal, logarithmic spatial (centered and uncentered), spatial, and encircled energy diagram. Along with this

numeric data concerning the temporal and spatial full width half max (FWHM) and percent of total energy encircled are given. A number of .txt files containing data are created, including information for the spatial, temporal, and encircled energy plots.

### III. Data Collection

Data was collected for errors of rotation around the vertical axis (TILT), rotation about the horizontal axis (TIP), rotation about the surface normal (IN-PLANE ROTATION), and grating distance mismatch using the program mantaray.

#### 3.1 TILT

A rotation about the vertical axis will introduce a grating alignment error that will affect the pulse shape. Figure 3.1.1 shows grating tilt.

A relationship between the amount of tilt and temporal broadening of the pulse can be observed when the Full Width at Half Max is plotted against the amount of error introduced to

the system. The tolerance limit, of 1 ps, is met at a tilt of 75  $\mu$ rad. The effect of tilt errors is independent of the grating that is misaligned, in that the effect of tilting the first grating 50  $\mu$ rad will be the same as tilting the second, third, or fourth. The results are shown in Figure 3.1.2.

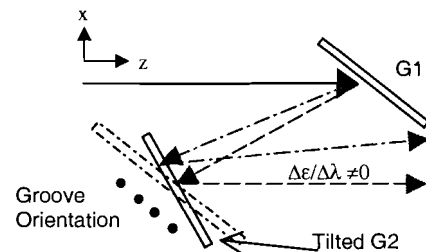


**Figure 3.1.1 Tilt of the Second Grating-** A rotation about the y-axis (groove orientation) causes an angular dispersion ( $\Delta\epsilon/\Delta\lambda$ ) in the x-z plane.

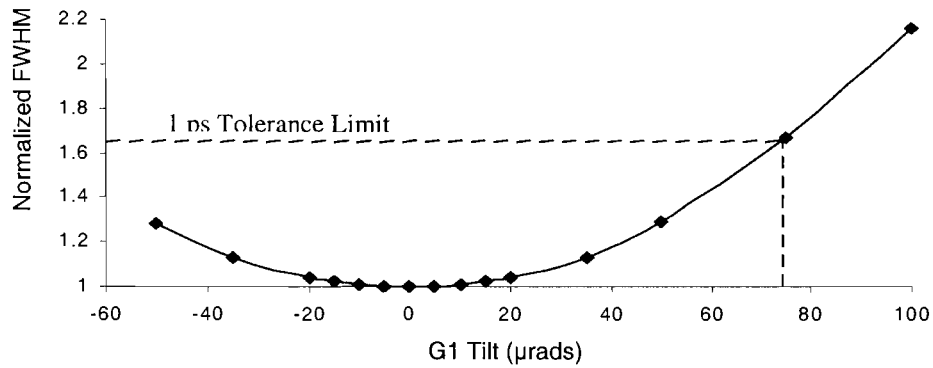


**Figure 3.1.2 Temporal FWHM Normalized to Transform-Limited FWHM for Grating Tilt-** Increasing the  $\mu\text{rad}$  of tilt, causes a broadening of the FWHM of the temporal pulse. A full width half max of 606 ps corresponds to a normalized FWHM of 1. The tolerance limit, of 1 ps, is met at a rotation of 75  $\mu\text{rad}$ .

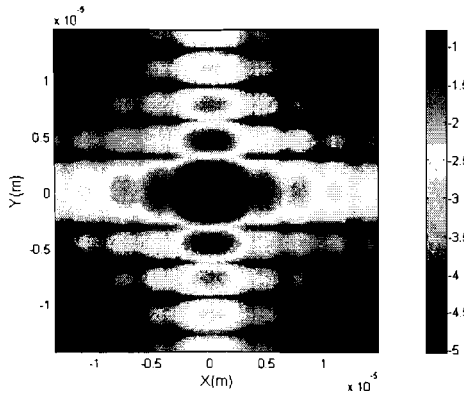


**Figure 3.1.3 Smearing in the X Direction Due to Grating Tilt-** The direction of angular dispersion for the far field of a grating tilt is orthogonal to the groove direction. Smearing in the x-direction is apparent in the far field of a 50  $\mu\text{rad}$  tilt of the first grating. The grooves run in the y-direction.

In the far field a similar effect is seen.

The focused beam for a tilt of the second grating will show smearing in the x-direction, which is the direction of residual angular dispersion.

Once again, as the amount of tilt is increased,

the smearing of the far field increases. An

example of the smearing caused by grating tilt is shown in Figure 3.1.3.

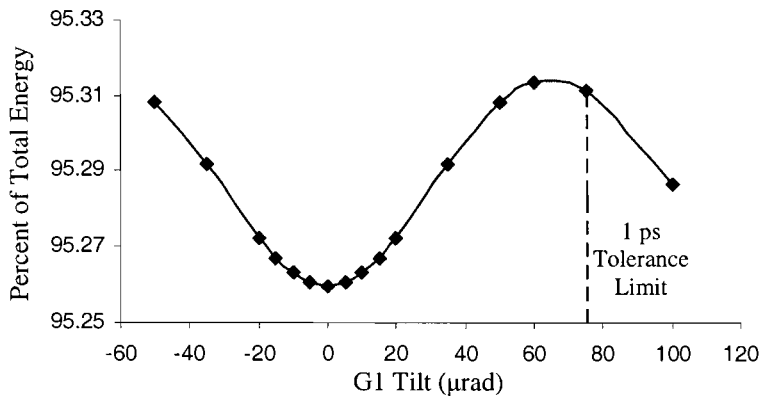


**Figure 3.1.5 Encircled Energy for a radius of 10  $\mu\text{m}$  for Grating Tilt-** The 80% encircled energy requirement for the laser system is met for all errors below the 1ps Tolerance Limit for Grating Tilt.

The amount of smearing that

is in the far field can be

found quantitatively using a

measurement of the pulse

width at the full width at half

max. This spatial FWHM

displays a relationship

similar to that of the

temporal FWHM.

A parabolic relationship between the amount of tilt introduced to the system and the spatial FWHM becomes readily apparent. This plot is shown in Figure 3.1.4. The

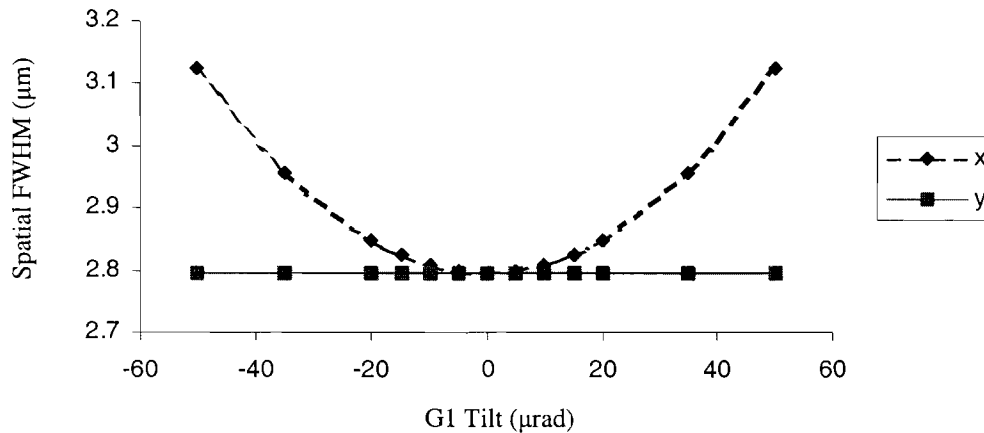


**Figure 3.1.4 Spatial FWHM Increases in the X-Direction-** The broadening of the spatial FWHM in the x-direction corresponds to the smearing seen in the far field of the beam. The relationship of spatial FWHM to error is similar to that of the temporal pulse.

laser system specifies that a circle of radius 10 μm must encircle 80% of the total energy that the beam contains. When the percent of total energy is plotted against the total amount of tilt error introduced to the system, it can be seen that the amount of energy for tilt errors less than the tolerance limit, provides more than 95% of the total energy meeting the standards set for the laser system. Figure 3.1.5 shows encircled energy for a circle of 1 μm for varying grating tilts

### 3.2 TIP

A rotation about the horizontal axis will introduce an angular dispersion in the y-z plane. Grating tip will also cause broadening of the pulse temporally and spatially. An example of Grating Tip is shown in Figure 3.2.1.

A grating tip will introduce temporal broadening as the amount of tip is increased. A plot of the temporal Full Width at Half Max vs. grating tip shows how a pulse can be broadened as the amount of error increases. For a broadening of 1 ps, which corresponds to the tolerance limit, the grating would need

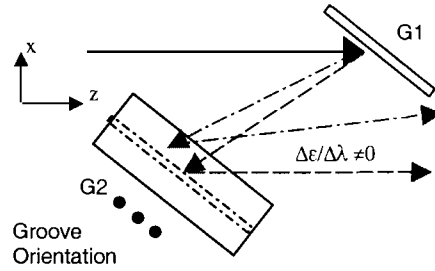


**Figure 3.2.1 Tip of the Second Grating-** A rotation about the x-axis of the grating, (orthogonal to the groove orientation) causes an angular dispersion ( $\Delta\epsilon/\Delta\lambda \neq 0$ ) in the y-z plane.

to be tipped 250  $\mu\text{rad}$ . The relationship between the temporal FWHM and grating tip is

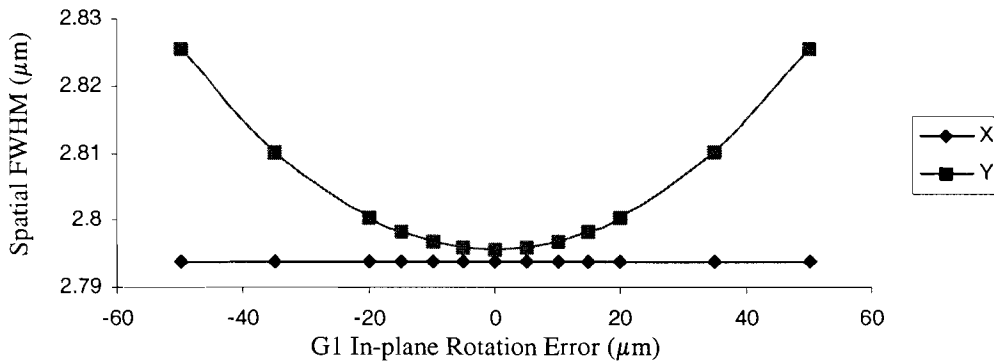


**Figure 3.2.4 Spatial FWHM Increases in the Y-Direction-** The broadening of the spatial FWHM in the y-direction corresponds to the smearing seen in the far field of the beam. The relationship of spatial FWHM to error is similar to that of the temporal pulse.

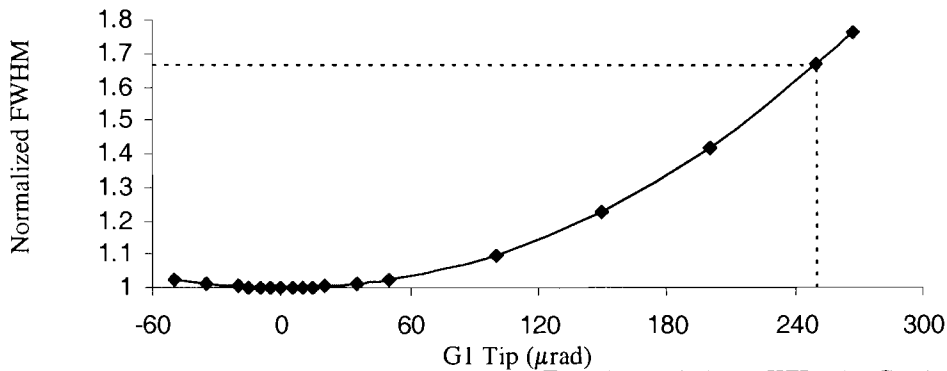


**Figure 3.2.2 Temporal FWHM Normalized to Transform-Limited FWHM for Grating Tip-** Increasing the  $\mu\text{rad}$  of tip, causes a broadening of the FWHM of the temporal pulse. The tolerance limit, of 1 ps, is met at a tip of 250  $\mu\text{rad}$ .

shown in figure 3.2.2.

Spatially the far field shows smearing in the y-direction, which is the direction of the residual angular dispersion. This angular dispersion is along the groove orientation, and orthogonal to the smearing that is apparent from a grating tilt misalignment. Figure 3.2.3 shows an angular dispersion of the far field for a grating tip of  $250 \mu\text{rad}$ , which corresponds to the 1 ps tolerance limit that is required by the laser system.

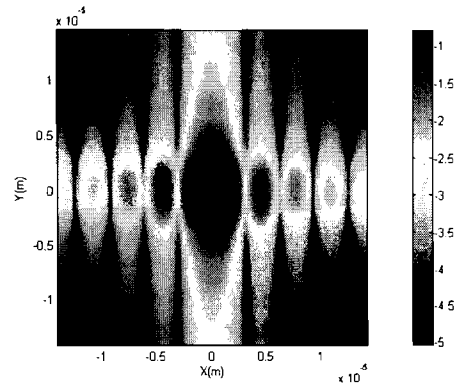


**Figure 3.2.3 Smearing in the Y Direction Due to Grating Tip-** The direction of angular dispersion for the far field of a grating tip is along the groove direction. Smearing in the y-direction is apparent in the far field of a  $267 \mu\text{rad}$  tip of the first grating.

The required 80% of encircled energy is met for all tip errors that fall below the 1 ps tolerance limit. Figure 3.2.4 shows the encircled energy for different amounts of tip error.

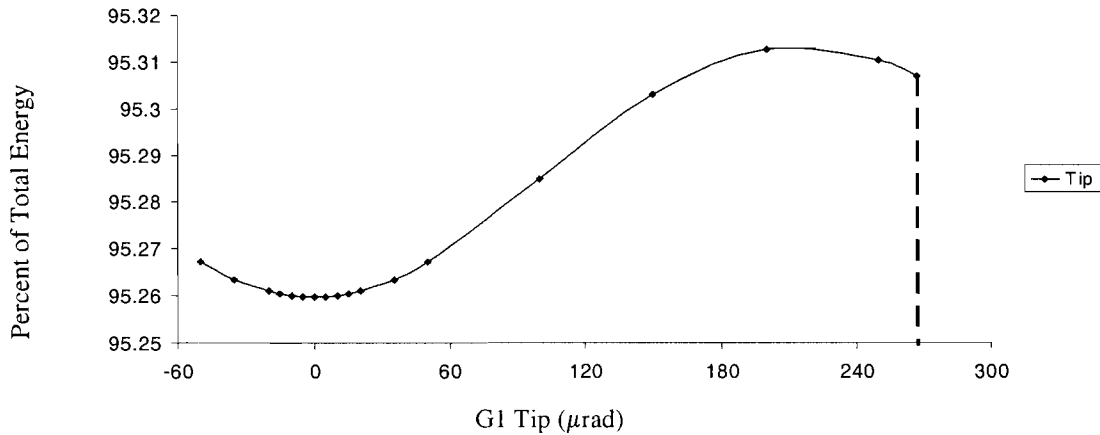


**Figure 3.2.5 Encircled Energy for a radius of  $10 \mu\text{m}$ -** The 80% encircled energy requirement for the laser system is met for all errors below the 1ps Tolerance Limit.

### 3.3 IN-PLANE ROTATION

A rotation about the axis normal to the grating face will cause smearing in the y-z plane much like a grating tip. Figure 3.3.1 shows a grating rotation.

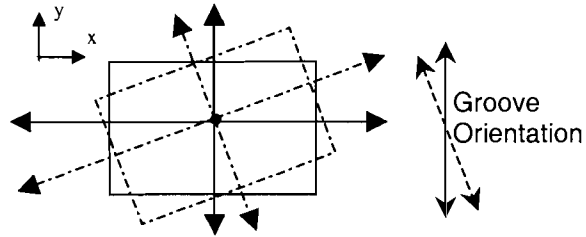


**Figure 3.3.1 In-plane rotation of the Second Grating-** A rotation about the z-axis of the grating, causes an angular dispersion ( $\Delta\epsilon/\Delta\lambda$ ) in the y-z plane, and alters groove orientation.

Temporal broadening will

increase as the amount of rotation increases. A plot of the FWHM of a pulse for varying in-plane rotation errors shows this correlation (Figure 3.3.2). A broadening of 65%, which corresponds to the 1 ps tolerance limit, is met at an in-plane rotation of 450  $\mu\text{rad}$ .

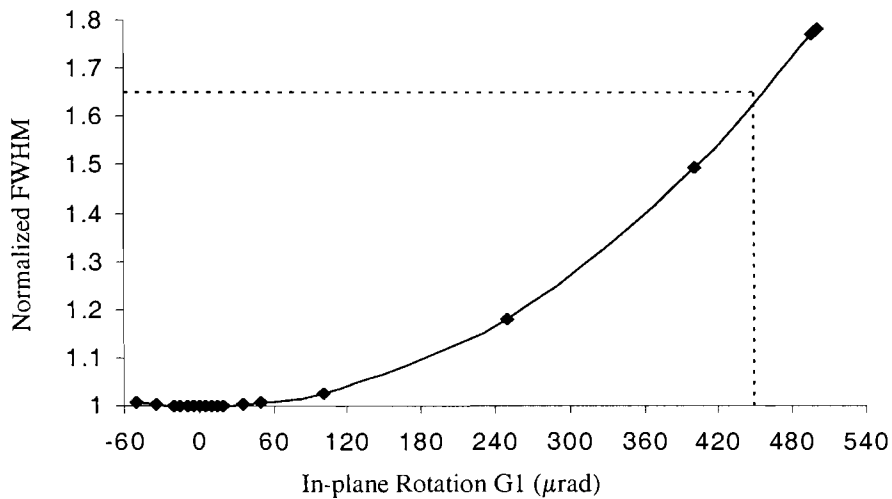


**Figure 3.3.2 Temporal FWHM Normalized to Transform-Limited FWHM for Grating In-plane Rotation-** Increasing the  $\mu\text{rad}$  of in-plane rotation, causes a broadening of the FWHM of the temporal pulse. The tolerance limit, of 1 ps, is met at a rotation of 450  $\mu\text{rad}$ .

Spatial broadening exhibits similar behavior to grating tip. Angular dispersion in the y-z plane causes smearing the y-direction. This smearing is visible in the far field of the beam. Figure 3.3.3 shows a far field for a 450  $\mu\text{rad}$  rotation. Numerically the spatial FWHM shows broadening the y-direction, similar to the effect seen in a grating tip. The

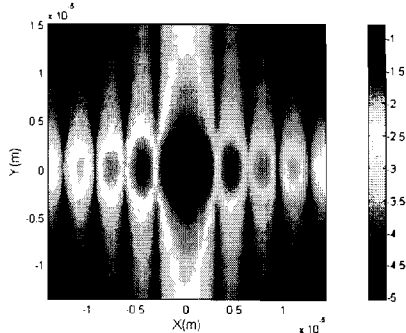


**Figure 3.3.3 Smearing in the Y Direction Due to Grating In-plane Rotation-** The direction of angular dispersion for the far field of a grating in-plane rotation is along the groove direction. Smearing in the y-direction is apparent in the far field of a 450  $\mu\text{rad}$  rotation of the first grating, which corresponds to the 1 ps tolerance limit.

80% total energy requirement is met for all rotations

that are less than the tolerance limit of 250  $\mu\text{rad}$ .

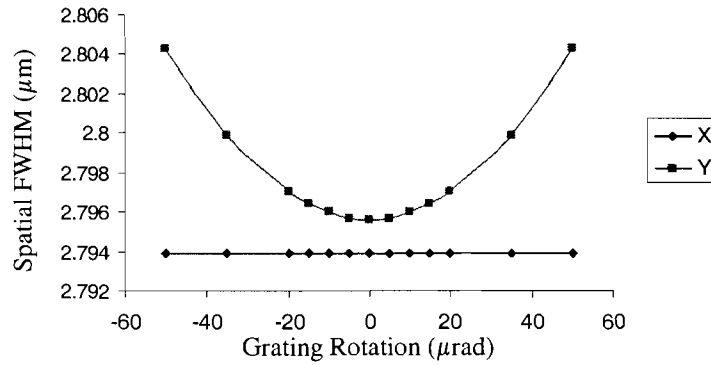


**Figure 3.3.4 Spatial FWHM Increases in the Y-Direction-** The broadening of the spatial FWHM in the y-direction corresponds to the smearing seen in the far field of the beam. The relationship of spatial FWHM to error is similar to that of the temporal pulse.

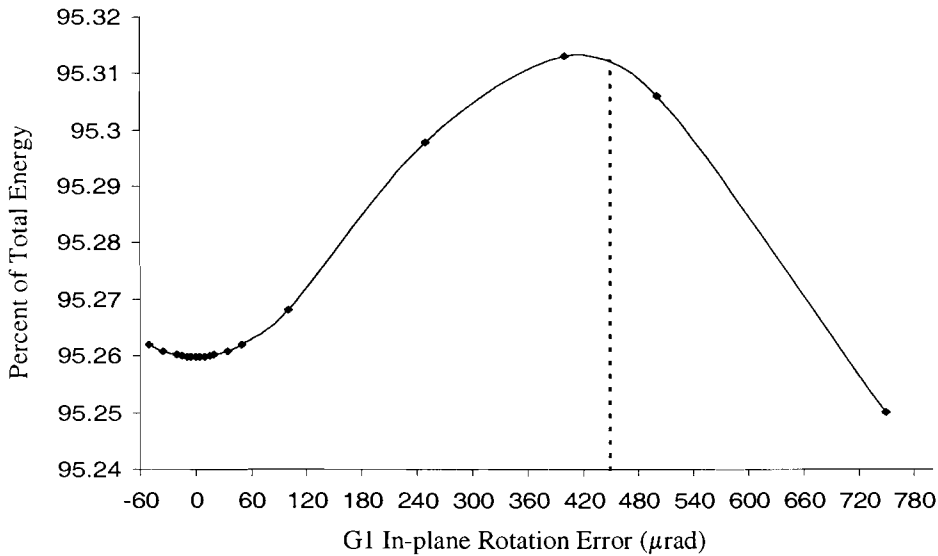


**Figure 3.3.5 Encircled Energy for a radius of 10  $\mu\text{m}$ -** The 80% encircled energy requirement for the laser system is met for all errors below the 1ps Tolerance Limit.

### 3.4 Grating Distance Mismatch

Changing the distance between gratings without changing orientation will cause a broadening of the temporal pulse. No angular dispersion is induced, however.

Figure 3.4.1 shows Grating Distance Mismatch.

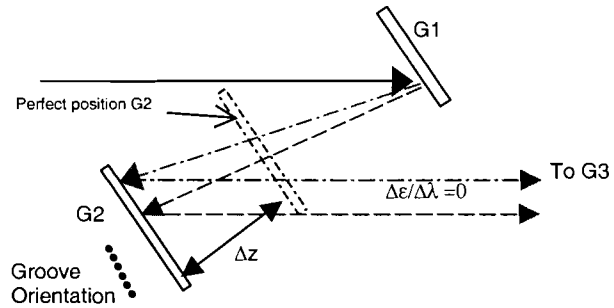


**Figure 3.4.1 Grating Distance Mismatch of the Second Grating-** Shifting the grating straight back causing a temporal broadening. Angular dispersion ( $\Delta\epsilon/\Delta\lambda$ ) is not induced and therefore equals zero.

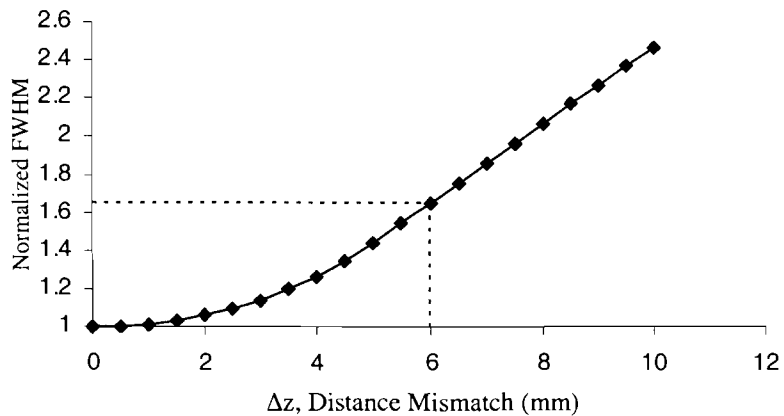


**Figure 3.4.2 Temporal FWHM Normalized to Transform-Limited FWHM for Grating Distance Mismatch-** Increasing the distance between gratings causes a temporal broadening. The tolerance limit of 1 ps is met at a grating distance mismatch of 6mm.

Temporally the relationship between the FWHM and the amount of distance mismatch appears to start out as a hyperbolic curve and eventually reach a linear relationship. Figure 3.4.2 shows the relationship between grating distance mismatch and pulse width.

Since there is no residual angular dispersion, the far fields of grating distance mismatches show no smearing. A comparison of the far field for a perfect compressor alignment and a compressor with a second grating displaced 9 mm shows no difference.

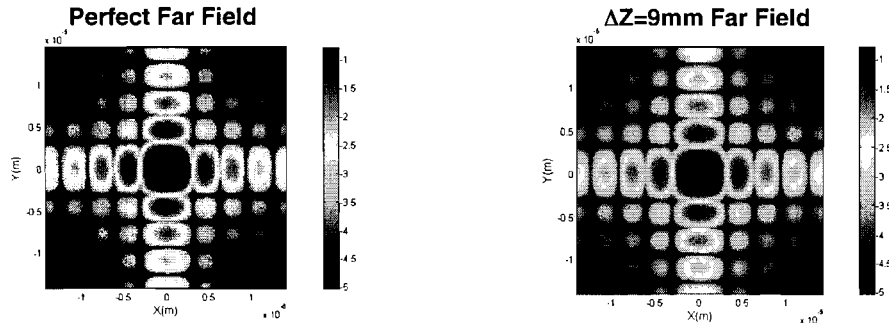


**Figure 3.4.3 Far Field of Grating Distance Mismatch-** Since there is not residual angular dispersion, the far field of a grating distance mismatch shows no smearing. The far field on the right shows no smearing for a grating distance mismatch of 9 mm.

## IV. Discussion

### 4.1 Angular Error Comparison

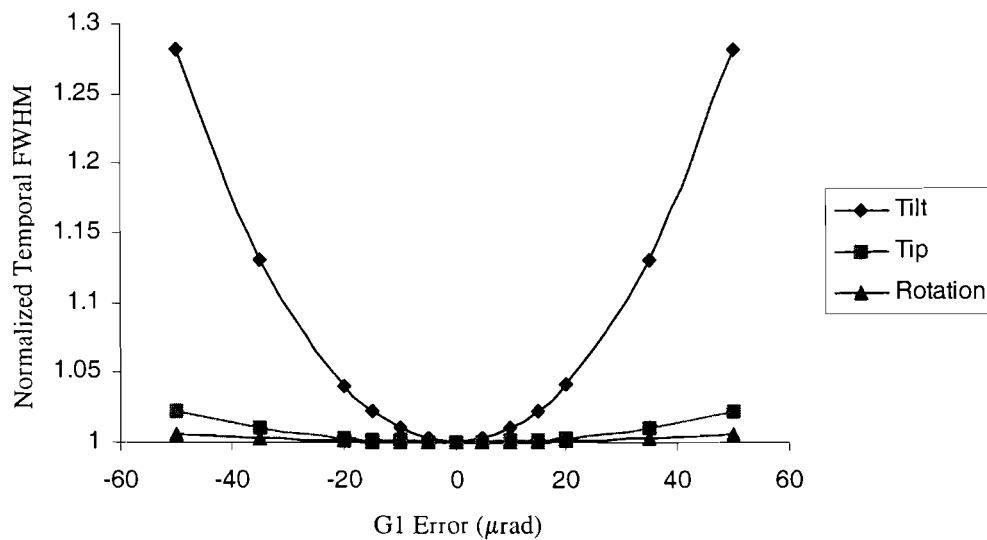


**Figure 4.1.1 Comparison of Angular Errors Temporal Effects-** A comparison of the broadening caused by angular errors shows that a tilt error has the greatest effect on pulse width.

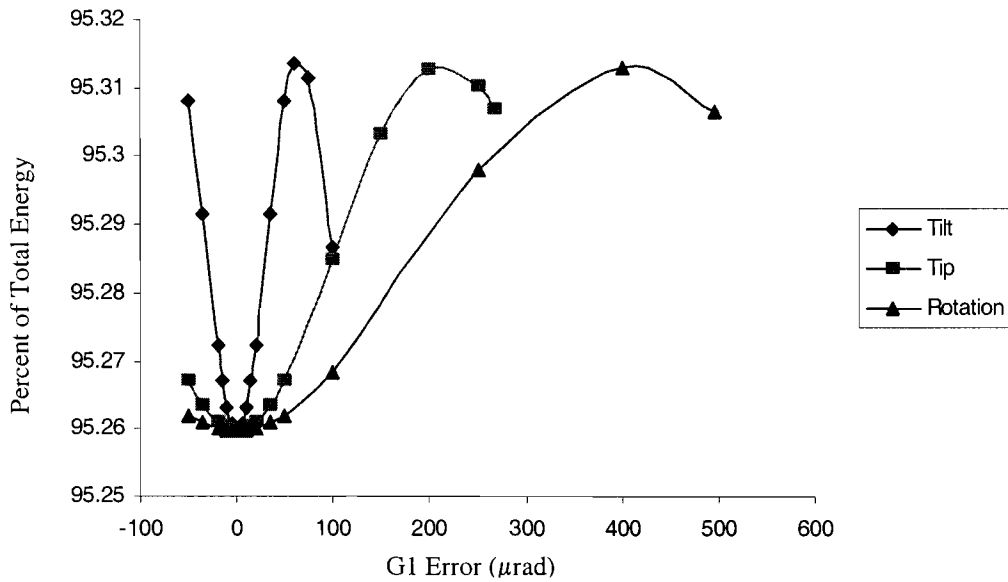


**Figure 4.1.2 Comparison of Angular Errors Encircled Energy-** A comparison of the encircled energy plots, shows that spatially tilt errors have the greatest effect, since the change in energy is more rapid. Percent energy is encircled in a circle of radius 20 μm

A comparison of angular errors shows that tilt errors have the greatest effect temporally and spatially, and then tip error, and finally in-plane rotation. This fits with the temporal tolerance limits of tilt, tip, and in-plane rotation, which are 75 μrad, 250μrad, and 450 μrad respectively.

A comparison of the angular errors encircled energy plots shows that spatially the effect caused by tilt is the greatest. For all angular errors, however, the 80% encircled energy requirement is met. Figure 4.1.1 shows the comparison of angular errors temporal pulse width and Figure 4.1.2 shows the comparison of angular errors encircled energy.

## 4.2 Temporal Broadening

Broadening of the temporal pulse is caused by a pulse front tilt introduced to the beam by the grating alignment error. This pulse front tilt can be calculated using the equation

$$\tan \gamma = \omega \frac{\delta\theta}{\delta\omega}$$

where  $\gamma$  is the angle of pulse front tilt and  $\delta\theta/\delta\omega$  corresponds to the angular dispersion [3]. This pulse front tilt causes a shift in time of each spatial location in the beam. When these separate pulses are added together, the spatially integrated temporal pulse shows a broadening.

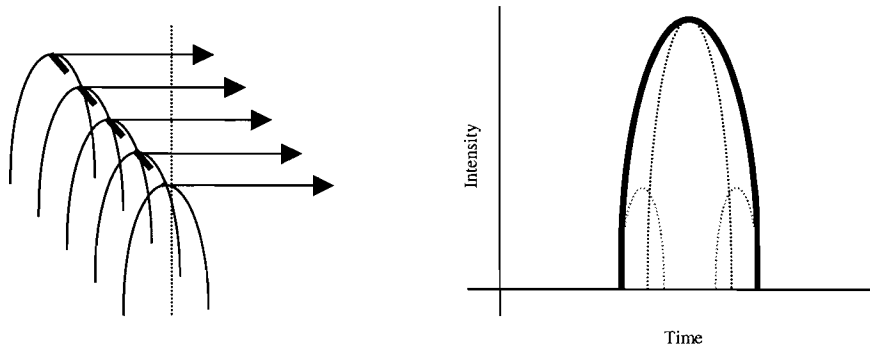


**Figure 4.2.1 Temporally Integrated Pulse-** When a pulse front tilt (shown on the left) is introduced spatial points are shifted in time. When the spatial points are integrated (shown on the right) the integrated pulse shows broadening.

### 4.3 Compensation

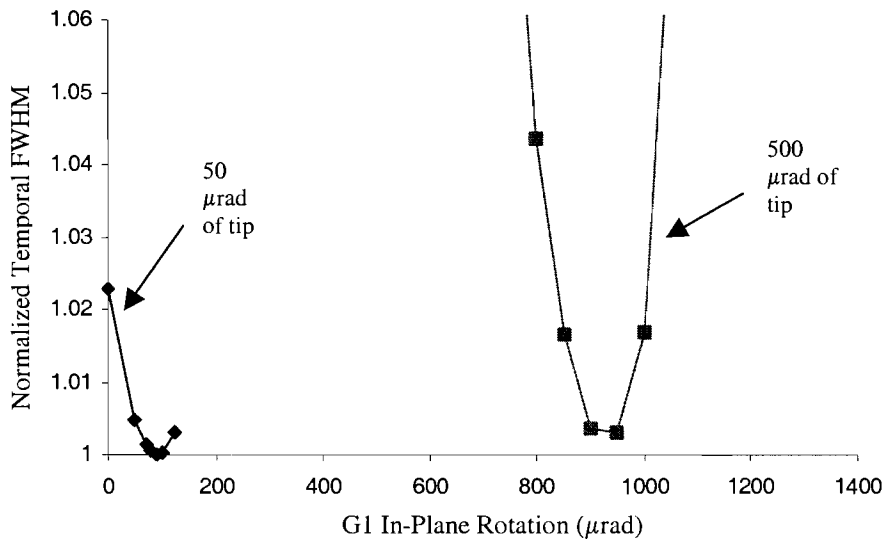


**Figure 4.3.1 Compensation of 50 μrad and 500 μrad tip-** Grating Tip can be compensated using in-plane rotations. Each curve represents a different amount of tip. Notice that the 50 μrad curve leaves the transform limit shown as 1.

Since the broadening of a pulse is caused by the shift in time of spatial locations in-plane rotation can be used to compensate tip errors. This works only for small errors, however, since large angular errors introduce a certain degree of distance mismatch. Figure 4.3.1 shows the compensation of a small tip compared to a larger tip. Figure 4.3.2 shows an even larger tip.

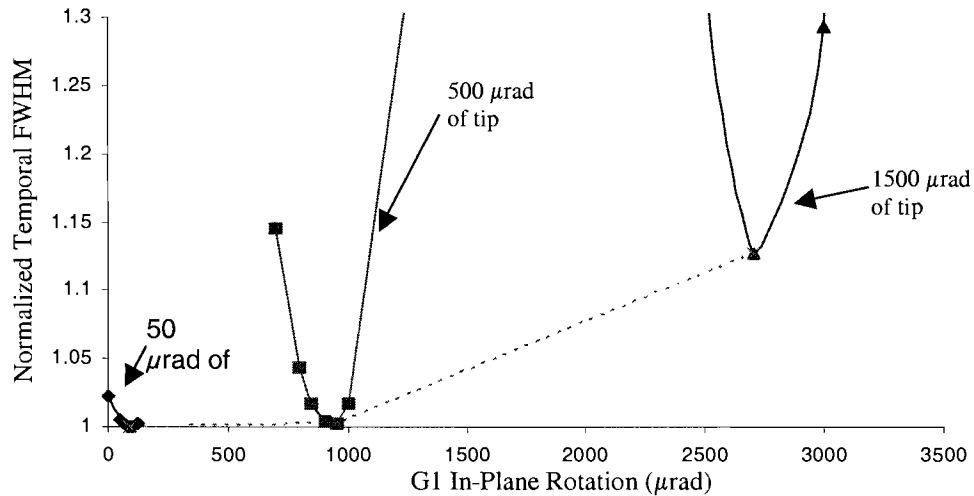


**Figure 4.3.2 Compensation of 50 μrad, 500 μrad, and 1500 μrad tip-** The larger the amount of tip the harder it is to compensate. Compared to a 50 μrad tip and 500 μrad tip a 1500 μrad is not broadened. The curve for the 1500 μrad tip floats above the transform limit of 1.

#### 4.4 Angular Dispersion

A perfect compressor alignment will output spatial rays that are parallel to each other. As error is introduced to the system, however, residual angular dispersion causes the rays to not be parallel. Angular dispersion can be found by taking the change in angle between wavelengths and dividing that by change in wavelength. When the wavelengths are integrated into the far field, smearing occurs.

## 4.5 Encircled Energy

Careful inspection of the encircled energy diagrams for a circle of radius  $10\ \mu\text{m}$  reveals an unexplained initial rise in encircled energy. A comparison of angular errors encircled energy vs. radius curve shows a rippling affect. This can be attributed to the modulations that occur in the far field, since the input pulse is not a Gaussian.

Introduction of an angular error smoothes the encircled energy diagram. Figure 4.5.1 shows a comparison of  $100\ \mu\text{rad}$  tilt of the first grating and a perfect grating alignment encircled energy diagram.

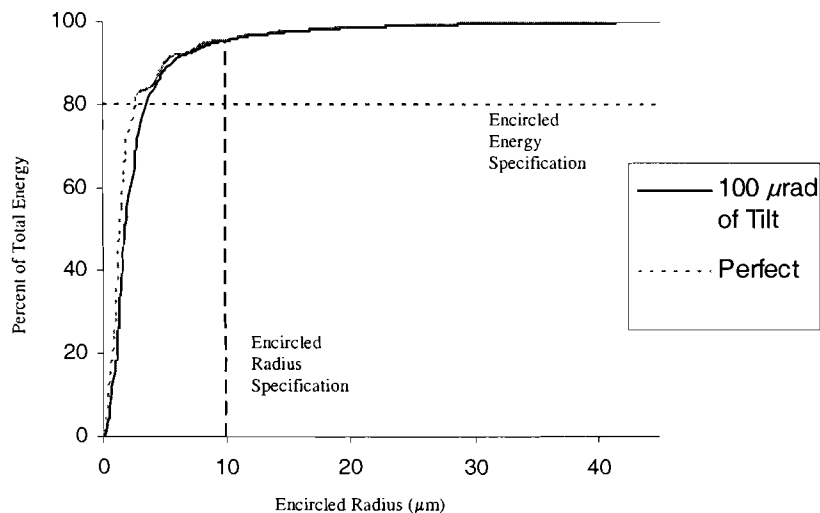


**Figure 4.5.1 Comparison of Encircled Energy Diagrams-** A comparison of the encircled energy diagrams for a perfect alignment and a tilted  $g_1$  of  $100\ \mu\text{rad}$ , shows how the curve smoothes as error is introduced.

The smoothing of the curve causes the diagram for errors to dip below the perfect grating alignment. This, however, is limited to very small increments as a circle of radius  $9.0\ \mu\text{m}$  or  $11.0\ \mu\text{m}$  encircles less energy for errors (see Figure 4.5.2). Eventually,

however, the smoothing of the curve for larger errors causes the encircled energy to fall

below

the

perfect

case.

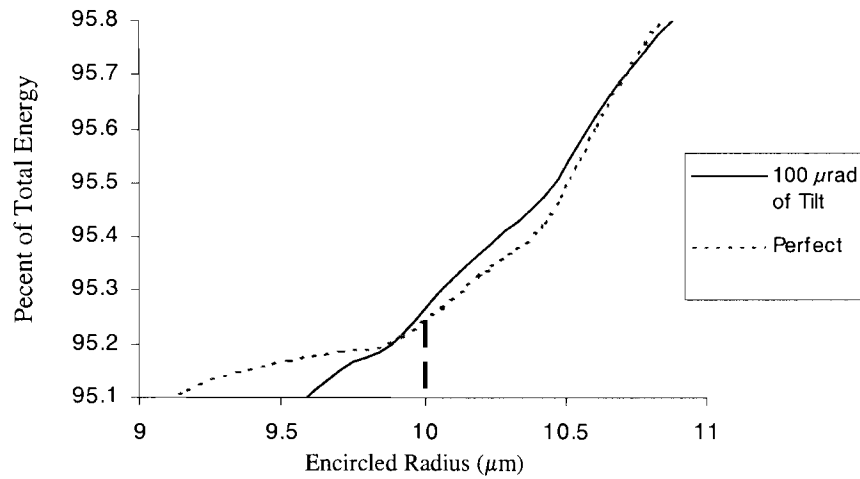


**Figure 4.5.2 Comparison of Encircled Energy Diagrams-** A closer look at the specified radius shows that the rippling effect causes the rise in encircled energy.

## V. Conclusion

Misalignments in the grating compressor system cause broadening of the laser pulse. A 1 ps pulse width can be achieved by displacing the gratings 6 mm, or tilting the grating 75  $\mu\text{rad}$ , or tipping the grating 250  $\mu\text{rad}$ , or rotating the grating 450  $\mu\text{rad}$ .

Spatially smearing occurs. However, the requirement of 80% of the total energy to be contained within a circle of a radius of 1  $\mu\text{m}$  is met for all errors that correspond to the 1 ps tolerance limit.



## **VI. Acknowledgement**

I would like to thank Dr. Stephen Craxton for the opportunity to work at the University of Rochester Laboratory for Laser Energetics, as well as my advisor Mark Guardalben, and George Dahl and Joshua Keegan for their work on the program MANTARAY.

## **VI. References**

- [1] D. Strickland and G. Mourou, "Compression of Amplified Chirped Optical Pulses," *Opt. Commun.* 56, 219 (1985).
- [2] E.B. Treacy, "Optical Pulse Compression With Diffraction Gratings," *IEE J. of Quantum Electronics*, vol. QE-5, pp 454-458, September 1969.
- [3] K.Osvay, A. P. Kovács, Z. Heiner, G. Kurdi. J. Klebniczki, and M. Csatári, "Angular Dispersion and Temporal Change of Femtosecond Pulses From Misaligned Pulse Compressors," *IEEE J. of Quantum Electronics*, vol. 10, pp 213-220, September 2004.

## **VI. Acknowledgement**

I would like to thank Dr. Stephen Craxton for the opportunity to work at the University of Rochester Laboratory for Laser Energetics, as well as my advisor Mark Guardalben, and George Dahl and Joshua Keegan for their work on the program MANTARAY.

## **VI. References**

- [1] D. Strickland and G. Mourou, "Compression of Amplified Chirped Optical Pulses," *Opt. Commun.* 56, 219 (1985).
- [2] E.B. Treacy, "Optical Pulse Compression With Diffraction Gratings," *IEEE J. of Quantum Electronics*, vol. QE-5, pp 454-458, September 1969.
- [3] K.Osvay, A. P. Kovács, Z. Heiner, G. Kurdi. J. Klebniczki, and M. Csatári, "Angular Dispersion and Temporal Change of Femtosecond Pulses From Misaligned Pulse Compressors," *IEEE J. of Quantum Electronics*, vol. 10, pp 213-220, September 2004.